

# Using the Lund-Potsdam-Jena Model to Understand the Different Responses of Three Woody Plants to Land Use in China

SUN Guodong\*<sup>1</sup> (孙国栋) and MU Mu<sup>2,1</sup> (穆穆)

<sup>1</sup>*State Key Laboratory of Numerical Modeling for Atmospheric Sciences and Geophysical Fluid Dynamics, Institute of Atmospheric Physics, Chinese Academy of Sciences, Beijing 100029*

<sup>2</sup>*Key Laboratory of Ocean Circulation and Wave, Institute of Oceanology, Chinese Academy of Sciences, Qingdao 266071*

(Received 9 February 2012; revised 12 June 2012)

## ABSTRACT

In this study, the approach of conditional nonlinear optimal perturbation related to initial perturbation (CNOP-I) was employed to investigate the maximum variations in plant amount for three main woody plants (a temperate broadleaved evergreen, a temperate broadleaved summergreen, and a boreal needleleaved evergreen) in China. The investigation was conducted within a certain range of land use intensity using a state-of-the-art Lund-Potsdam-Jena dynamic global vegetation model (LPJ DGVM). CNOP-I represents a class of deforestation and can be considered a type of land use with respect to the initial perturbation. When deforestation denoted by the CNOP-I has the same intensity for all three plants, the variation in plant amount of the boreal needleleaved evergreen in northern China is greater than the variation in plant amount of both the temperate broadleaved evergreen and temperate broadleaved summergreen in southern China. As deforestation intensity increases, the plant amount variation in the three woody plant functional types carbon changes, in a nonlinear fashion. The impact of land use on plant functional types is minor because the interaction between climate condition and land use is not considered in the LPJ model. Finally, the different impacts of deforestation on net primary production of the three plant functional types were analyzed by modeling gross primary production and autotrophic respiration. Our results suggest that the CNOP-I approach is a useful tool for exploring the nonlinear and different responses of terrestrial ecosystems to land use.

**Key words:** conditional nonlinear optimal perturbation, initial perturbation, CNOP-I, terrestrial ecosystem, land use

**Citation:** Sun, G. D., and M. Mu, 2013: Using the Lund-Potsdam-Jena model to understand the different responses of three woody plants to land use in China. *Adv. Atmos. Sci.*, **30**(2), 515–524, doi:10.1007/s00376-012-2011-1.

## 1. Introduction

Land use has had severe effects on the Earth. More than one-third of the global land surface has been transformed through anthropogenic activities such as deforestation, agriculture and grazing (Vitousek et al., 1997). Since the year 1700, global forest cover has been reduced by seven to ten million square kilometers as a result of land use activities. During the last 40 years of the twentieth century, irrigated cropland areas increased by ~70% (Foley et al., 2005). These changes

in land use have resulted in increases in both land albedo and atmospheric CO<sub>2</sub> (Betts and Ball, 1997; Sitch et al., 2005). This CO<sub>2</sub> increase can seriously affect global climate and environmental conditions, such as drought, heat islands and air quality. Hence, land use and land use changes play key roles in global environment (Vitousek et al., 1997; Claussen et al., 2001; Brovkin et al., 2004).

The impact of land use and land use changes on terrestrial ecosystems and the carbon cycle has been widely studied in the field of global ecosystems and en-

---

\*Corresponding author: SUN Guodong, sungd@mail.iap.ac.cn

vironment. Some international institutions have collected land use data and measured the response of terrestrial ecosystems to land use. For example, the Land Use/Cover Change (LUCC) project (Lambin and Geist, 2006) and Global Land Project (GLP, 2005) have focused on reconstruction of historical land use and land cover. The Global Carbon Project (GCP, 2003) emphasizes, in particular, the impact of human activities on terrestrial ecosystems. Other studies have quantified the influence of land use on the global carbon cycle (Houghton, 1995; Petit and Lambin, 2002; Houghton and Hackler, 2003). Houghton (1995) showed that  $\sim 123$  Pg of carbon was released into the atmosphere due to land use from 1850 to 1980. In the 1980s,  $\sim 1.6 \pm 0.7$  Pg of carbon attributable to land use was emitted to the atmosphere, most of which was derived from equatorial regions. Land use affects not only atmospheric  $\text{CO}_2$ , but also carbon reserves in terrestrial ecosystems. A net emission of  $\text{CO}_2$  to the atmosphere from mineral soils of 46.4 Tg for the period 1975–1995 was attributed to land use in Brazil (Bernoux et al., 2001). Another studies have reported that the soil carbon reserves of global grasslands were augmented as a result of protecting grasslands and managing grazing appropriately (Conant et al., 2001; Conant and Paustian, 2002; Piao et al., 2007; Solomon et al., 2007).

China comprises a great variety of terrestrial ecosystems that have undergone significant changes as a result of human activities such as deforestation and farming (Piao et al., 2007; Ge et al., 2008). Prior the 1950s, the forested area in China was reduced by 50%, while plantation areas rapidly increased (Ge et al., 2008). Fang et al. (2001) clearly showed that forested areas were augmented due to government management since the 1970s. The impact of land use on the carbon cycle of terrestrial ecosystems is severe. Houghton and Hackler (2003) found that a decrease in forested areas was the main cause for net emissions of carbon to the atmosphere. However, this carbon source was converted to carbon sink in China due to effective management of forested areas (Fang et al., 2001; Ge et al., 2008). Decreases in soil carbon have been attributed to land use in arid and semi-arid regions from northeastern China to southwestern China (Gao et al., 2003; Wu et al., 2003). Although there are many studies of the influence of land use and its change on terrestrial ecosystems, results vary depending on whether they were based on observation data and/or vegetation models (Houghton and Hackler, 2003). For example, the forest area in 1700 was reported to be  $\sim 248 \times 10^6$   $\text{hm}^2$  by Ge et al. (2008), but it was reported to be  $322 \times 10^6$   $\text{hm}^2$  by Houghton and Hackler (2003). These difference make it difficult to assess

forested areas as carbon source or sink, and the estimation of carbon in terrestrial ecosystems remains uncertain (Ge et al., 2008; Quaife et al., 2008). Furthermore, overall research on the maximum variation in plant amount caused by changes in land use remains scarce in China.

In this study, we investigate how plant amount in three plant functional types in China varies with land use. We employed the method of conditional nonlinear optimal perturbation related to initial perturbation (CNOP-I; Mu et al., 2003, 2010). CNOP-I is a type of perturbation that maximizes the cost function for a given physical constraint and optimization time. CNOP-I represents a kind of deforestation and, for the purposes of our work, can be considered a type of land use from the perspective of the initial perturbation. This approach has been applied to investigate the dynamics of ENSO predictability, prediction error (Mu et al., 2003), the nonlinear stability of steady states of thermohaline circulation (Mu et al., 2004), ensemble prediction (Mu and Jiang, 2008; Jiang and Mu, 2009) and adaptive observation (Mu et al., 2009). Mu and Wang (2007) used the approach to study the stability of grasslands. Sun and Mu (2009) built upon Mu and Wang's (2007) study and found that the equilibrium states are nonlinear. These studies illustrate that the CNOP-I approach is a useful tool for studying nonlinear ecosystems. However, because the model applied by Mu and Wang's (2007) study is simple, it is not applicable to terrestrial ecosystems in China. As such, a state-of-the-art dynamic global vegetation model (DGVM), Lund-Potsdam-Jena (LPJ, Sitch et al., 2003), was applied in this study.

## 2. The model and method

### 2.1 The LPJ model

The DGVM is an effective way to investigate the impacts of climate change on terrestrial ecosystems (Cramer et al., 2001; Bonan et al., 2003). The LPJ DGVM was employed in this study due to its broad application in modeling both terrestrial carbon cycles and hydrological cycles (Beer et al., 2007; Jung et al., 2007; Sitch et al., 2005). The model, which originates from the BIOME model family (Prentice et al., 1992), simulates the distribution of plant functional types and combines process-based representations of terrestrial vegetation dynamics and land-atmosphere carbon and water exchanges. LPJ DGVM explicitly considers photosynthesis, mortality, fire disturbance and soil heterotrophic respiration. The model was described and evaluated in detail by Sitch et al. (2003).

We obtained monthly precipitation, temperature,

wet day frequency and cloud cover from a Climatic Research Unit (CRU) data set developed for the 1901–1998 period (Mitchell and Jones, 2005). This dataset was assembled based on climate data. The data are considered fairly credible, especially given the lack of observation data in some regions. Wen et al. (2006) indicated that the amount of precipitation from the CRU coincided with observed data from 160 stations over the 1951–2000 period in China and that the temperature variation was similar to other data. A data set of global atmospheric CO<sub>2</sub> concentrations was derived from the carbon cycle model, ice core measurements and atmospheric observations (Kicklighter et al., 1999). Soil texture data based on the Food and Agriculture Organization (FAO) soil data set (Zobler, 1986).

## 2.2 Conditional nonlinear optimal perturbation related to initial perturbation

Although many studies have demonstrated the CNOP-I method, we introduce the approach here for readers' convenience. Let  $M_\tau$  be the propagator of a nonlinear model from 0 to  $\tau$ . An initial perturbation,  $u_0$  is superposed on  $U_0$ , which is the initial condition with respect to a basic state  $U(\tau)$ .  $U(\tau)$  is a solution to the nonlinear model and satisfies  $U(\tau) = M_\tau(U_0, P)$  at time  $\tau$ .

For a chosen norm  $\|\bullet\|$ , an initial perturbation  $u_{0\delta}$  is called CNOP-I, if and only if

$$J(u_{0\delta}) = \max_{u_0 \in \Omega_\delta} J(u_0),$$

where

$$J(u_0) = \|M_\tau(U_0 + u_0) - M_\tau(U_0)\|.$$

$u_0 \in \Omega_\delta$  is a constraint for initial perturbations. To obtain the maximum value of the above optimization problem, a nonmonotone spectral projected gradient (SPG2, Birgin et al., 2000) was employed. The method applies the gradients, which are acquired using the definition of the gradient and of the cost function  $J$  with respect to  $u_0$ .

## 2.3 Experimental design

The potential plant functional types (PFTs) and most of the net primary production (NPP) are distributed in the north–south transect of eastern China (Ni and Zhang, 2000; Gao et al., 2003); thus, the study region is chosen: 40°–54°N, 118°–135°E and 20°–36°N, 103°–120°E, excluding Taiwan. The potential woody plants in the north–south transect of eastern China are respectively: a temperate broadleaved

evergreen tree (TeBE), a temperate broadleaved summergreen tree (TeBS), and a boreal needleleaved evergreen tree (BoNE). These three PFTs were the target of this study, rather than desert and grassland. Therefore, the three wood plants in the study region are discussed. The optimization period was 1961–1970 due to the data reliability. Equilibrium carbon pool and vegetation cover conditions are obtained by the LPJ model simulation beginning from bare ground and running more than a 1000 model years spin-up period. These equilibrium conditions were used as the initial conditions for the subsequent analyses.

Deforestation is one type of land use. Within the LPJ model, the variables contributing to plant quantity are primarily leaf mass ( $L_m$ ), sapwood mass ( $S_m$ ), heartwood mass ( $H_m$ ), and fine root mass ( $R_m$ ). The plant amount changes and the four variables are synchronously reduced as deforestation occurs. Perturbations  $l_m$ ,  $s_m$ ,  $h_m$ , and  $r_m$  indicate the amount of deforestation. The constraint conditions represent physical characteristics. For a given norm, the first constraint condition is

$$(l_{m0}^2 + s_{m0}^2 + h_{m0}^2 + r_{m0}^2) \leq \delta^2,$$

where  $\delta$  is a constraint condition parameter representing the extent of deforestation at the initial time.  $\delta$  is given 0.5, 0.6, 0.7, and 0.8 in the study, which is ~25%, 30%, 35%, and 40% of the whole plant amount. The variables  $l_{m0}$ ,  $s_{m0}$ ,  $h_{m0}$ , and  $r_{m0}$  are initial perturbations of leaf mass, sapwood mass, heartwood mass, and fine root mass, respectively. Next, the perturbations should satisfy the condition:

$$\frac{l_{m0}}{L_{m0}} = \frac{s_{m0}}{S_{m0}} = \frac{h_{m0}}{H_{m0}} = \frac{r_{m0}}{R_{m0}}.$$

The second constraint condition implies that when deforestation occurs, the amounts of leaf mass, sapwood mass, heartwood mass, and fine root mass will synchronously decrease. Because they are inseparable whole, the ratio of the amounts of perturbation of the four variables with deforestation to their amounts without deforestation should be equal.

## 3. Numerical results

### 3.1 The variation of the three PFTs

To quantify the impact of deforestation on the three PFTs, the relative change in plant amount being equivalent to the cost function was calculated using the following formula:

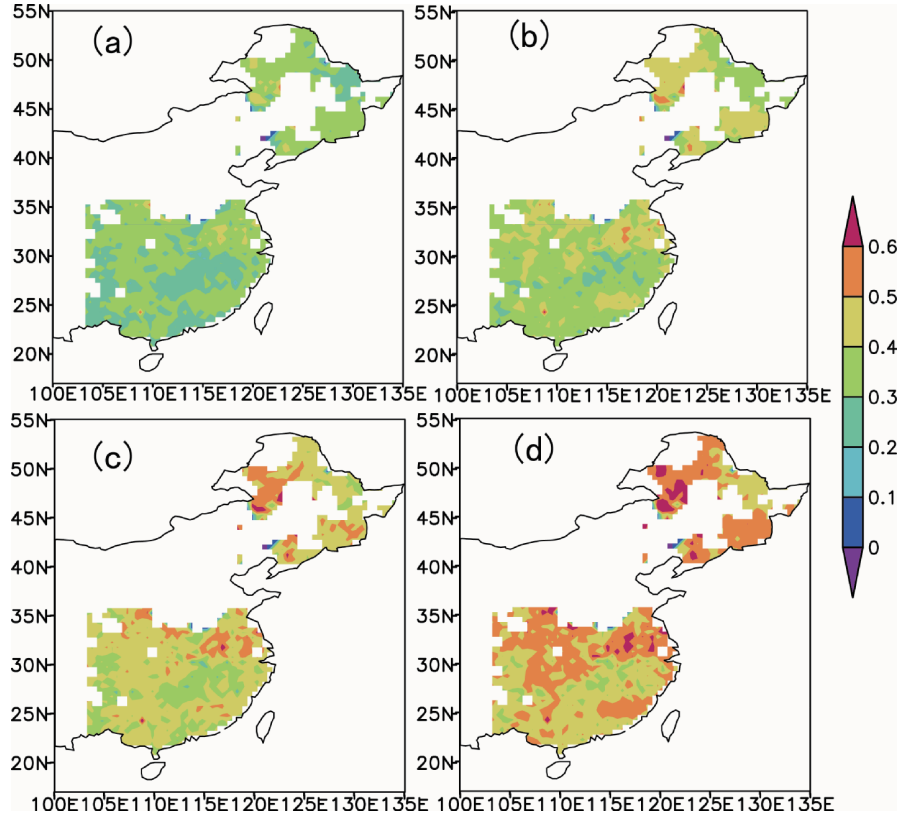


**Fig. 1.** Spatial distribution about the relative change in plant amount for three PFTs: (a)  $\delta=0.5$ , (b)  $\delta=0.6$ , (c)  $\delta=0.7$ , (d)  $\delta=0.8$ .

$$\sigma_i = \left[ \frac{(L_{mi}^* - L_{mi})^2 + (S_{mi}^* - S_{mi})^2 + (H_{mi}^* - H_{mi})^2 + (R_{mi}^* - R_{mi})^2}{L_{mi}^2 + S_{mi}^2 + H_{mi}^2 + R_{mi}^2} \right]^{\frac{1}{2}},$$

where  $i$  denotes year when there were CNOP-type land use. In the study,  $i$  is equal to 10 according to the optimization time. The larger the  $\sigma_i$ , the greater the relative change of the three plants is at a certain level of deforestation. The variables  $L_{mi}$ ,  $S_{mi}$ ,  $H_{mi}$ , and  $R_{mi}$  denote the values of the reference state in the  $i$ th year, which is obtained through integrating the LPJ model without initial conditions changing.  $L_{mi}^*$ ,  $S_{mi}^*$ ,  $H_{mi}^*$ , and  $R_{mi}^*$  are the outputs with the LPJ model using the changed initial condition that the CNOP-I is superimposed on the initial condition of the reference state in the  $i$ th year.

We find that the response of plant amount of the three plants to deforestation varies under the same constraint condition parameter (Fig. 1, Table 1). We observe much larger effects on plant amount in northern versus southern China. For example, the relative changes of BoNE, TeBS, and TeBE are 0.449, 0.431,

and 0.423, respectively, when  $\delta=0.7$ . The results were similar for other constraint condition parameters, and the relative changes increase as the constraint condition parameter increased. When the constraint condition parameter increases from 0.5 to 0.8, the TeBE

**Table 1.** Relative changes in plant amount for three plant functional types under different values of  $\delta$ .

$\delta$	TeBE	TeBS	BoNE
0.5	0.307	0.314	0.322
0.6	0.366	0.374	0.386
0.7	0.423	0.431	0.449
0.8	0.477	0.488	0.508

Note: TeBE, temperate broadleaved evergreen; TeBS, temperate broadleaved summergreen, and BoNE, boreal needleleaved evergreen tree.

increased from 0.307 to 0.477, the TeBS increased from 0.314 to 0.488 and the BoNE increases from 0.322 to 0.508. The variations in terms of the relative changes of each plant also display nonlinear characteristics.

Climate conditions play a key role in plant growth when deforestation occurs. Both photosynthesis and plant evapotranspiration are dependent on these climate conditions. During the study period, the average annual precipitation for BoNE, TeBS and TeBE were 571 mm, 917 mm, and 1354 mm, respectively, and the average annual temperature were 0.08°C, 12.73°C, and 16.97°C (Fig. 2), respectively. In southern China, precipitation is plentiful and the temperature is high, whereas in northern China, both precipitation and temperature are low. Our results demonstrate that the high availability of light and water favor increased growth of TeBE in southern China and that the response of TeBE to human activities and natural factors is relatively weak. In contrast, the low availability of light and water weaken the growth of BoNE in north-east China and BoNE is relatively sensitive to human activities and natural factors.

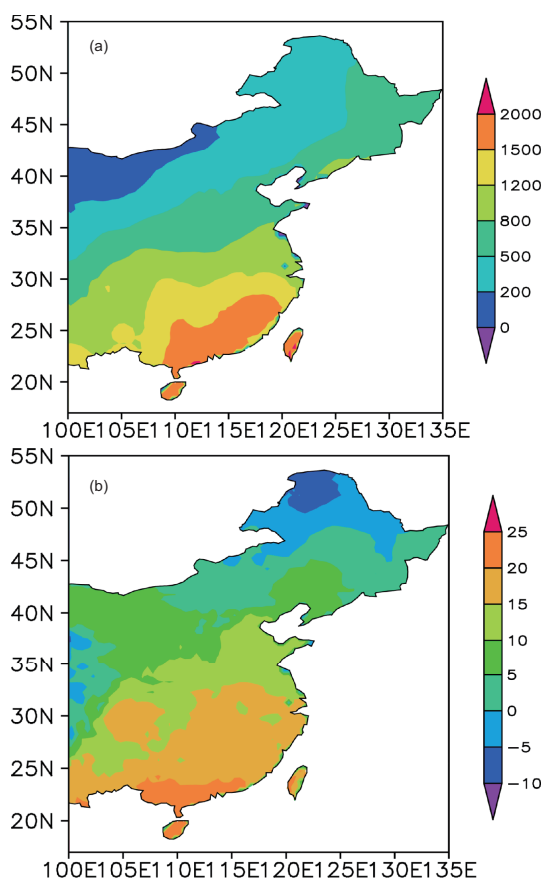


**Fig. 2.** Climate conditions during 1961–1970 in the study region: (a) precipitation (units: mm) and (b) temperature (units: °C).

**Table 2.** Average variation in net primary production for three plant functional types during 1961–1970 under different values of  $\delta$  (units:  $\text{g C m}^{-2} \text{ yr}^{-1}$ ).

$\delta$	TeBE	TeBS	BoNE
Reference state	559.27	514.21	453.68
0.5	596.23	544.81	474.61
0.6	605.23	552.03	479.16
0.7	614.14	559.35	483.84
0.8	622.76	566.65	488.21

**Table 3.** Same as in Table 2, but for gross primary production (units:  $\text{g C m}^{-2} \text{ yr}^{-1}$ ).

$\delta$	TeBE	TeBS	BoNE
Reference state	1519.48	1230.76	1037.41
0.5	1517.23	1241.81	1026.62
0.6	1516.72	1244.51	1023.36
0.7	1516.38	1247.07	1020.02
0.8	1516.37	1249.65	1015.90

### 3.2 Variations in NPP, GPP, and Ra

NPP is the net carbon gain by vegetation, which is the difference between gross primary production (GPP) and autotrophic respiration (Ra). NPP is a crucial variable in studies of the global carbon cycle and interactions between the atmosphere and terrestrial ecosystems (Dan et al., 2007). In our study, variation in NPP resulting from deforestation was analyzed over the period 1961–1970.

Across the whole region, total NPP increased during this period (Fig. 3), which is consistent with results of DeFries et al. (1999). While increases in NPP with the constraint condition parameter were similar for the three plants, the extent of variation differs among them (Table 2). When the constraint condition parameter was 0.5, the mean NPP of TeBE increases by  $36.96 \text{ g C m}^{-2} \text{ yr}^{-1}$ , which was  $6.4 \text{ g C m}^{-2} \text{ yr}^{-1}$  greater than that of TeBS. The variation of BoNE about the mean NPP was smaller than that of the other two plants. Results were similar for other constraint condition parameters. In terms of the relative change in NPP, the three plants show analogous variation (Fig. 4). For the same constraint condition parameter, the relative change in NPP in southern China was greater than the change in northern China. Across the whole region, the relative change gradually increased with the increasing of constraint condition parameter.

To analyze potential causes of variation in NPP, GPP, and Ra were also investigated because the LPJ model calculates NPP as the difference between GPP and Ra. The variations in total GPP for the three

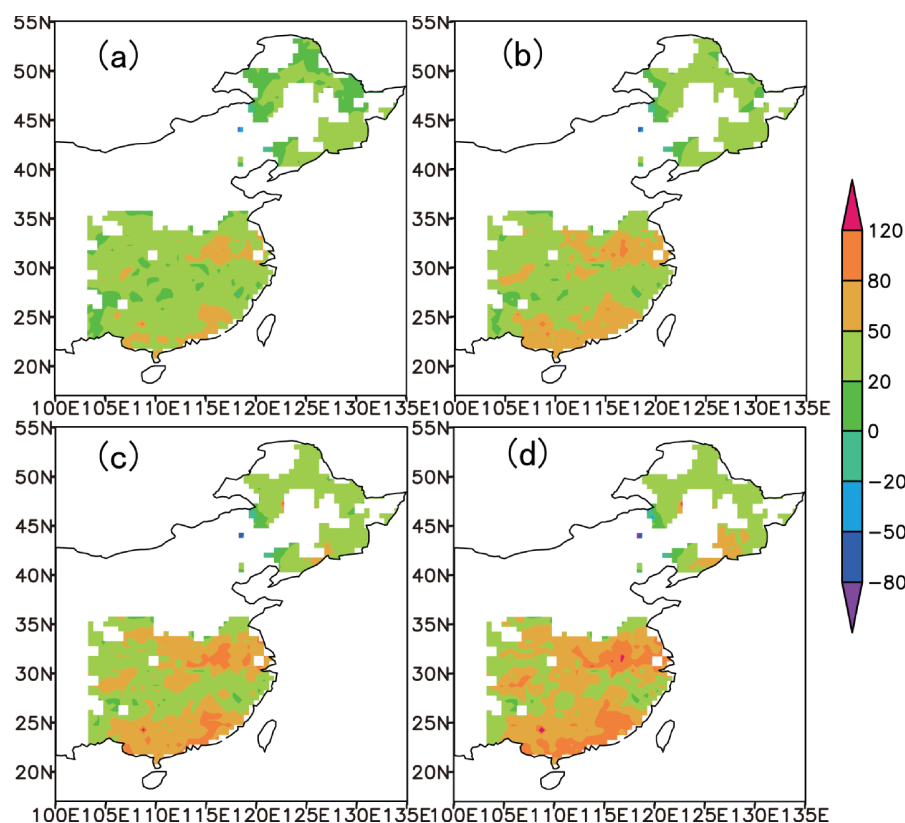


**Fig. 3.** Average variation in NPP during 1961–1970 (units:  $\text{g C m}^{-2} \text{ yr}^{-1}$ ): (a)  $\delta=0.5$ , (b)  $\delta=0.6$ , (c)  $\delta=0.7$ , (d)  $\delta=0.8$ .

PFTs display differences under the deforestation scenario (Fig. 5, Table 3). When  $\delta=0.5$ , GPP increases by  $11.05 \text{ g C m}^{-2} \text{ yr}^{-1}$  for TeBS, but was reduced by  $2.25 \text{ g C m}^{-2} \text{ yr}^{-1}$  for TeBE and by  $10.79 \text{ g C m}^{-2} \text{ yr}^{-1}$  for BoNE. The relative changes in GPP for the three PFTs were small, perhaps because variations in GPP are largely dependent on light and soil temperature and fairly insensitive to land use. The impact of deforestation on leaf carbon mass was also weak, so the variation in GPP was small. When deforestation occurred, variations in leaf, sapwood, heartwood and fine root carbon mass induce a reduction in Ra for the three PFTs (Fig. 6, Table 4). As the constraint condition parameter increase, the extent of variation is different for each of the three PFTs. When  $\delta=0.5$ , the average Ra was reduced by  $\sim 39.12 \text{ g C m}^{-2} \text{ yr}^{-1}$  for TeBE,  $\sim 19.45 \text{ g C m}^{-2} \text{ yr}^{-1}$  for TeBS and  $\sim 31.62 \text{ g C m}^{-2} \text{ yr}^{-1}$  for BoNE. These numerical results suggest that there were different reasons for the increase of NPP for each of the three plants. Both GPP and Ra were reduced for TeBE and BoNE, but NPP increased since the extent of decrease in GPP was less than that of Ra. However, in the case of TeBS, NPP increased because GPP increased and Ra decreased.

#### 4. The variation in PFTs

The impact of deforestation on plant vegetation type was also explored because different plant types can severely influence terrestrial ecosystems and carbon cycling (DeFries et al., 1999). Within the LPJ model, an important variable in determining plant type is foliage projective cover. The dominant plant was confirmed according to the highest simulated areal cover represented by the plant cover. The plant cover was related to the leaf area index, which depends on leaf carbon mass.

Results show that the plants in the study region were unaltered except for a small part of northeast

**Table 4.** Same as in Table 2, but for autotrophic respiration (units:  $\text{g C m}^{-2} \text{ yr}^{-1}$ ).

$\delta$	TeBE	TeBS	BoNE
Reference state	960.67	719.73	589.50
0.5	921.55	700.28	557.88
0.6	912.06	695.80	550.10
0.7	902.84	691.06	542.12
0.8	894.25	686.36	533.69

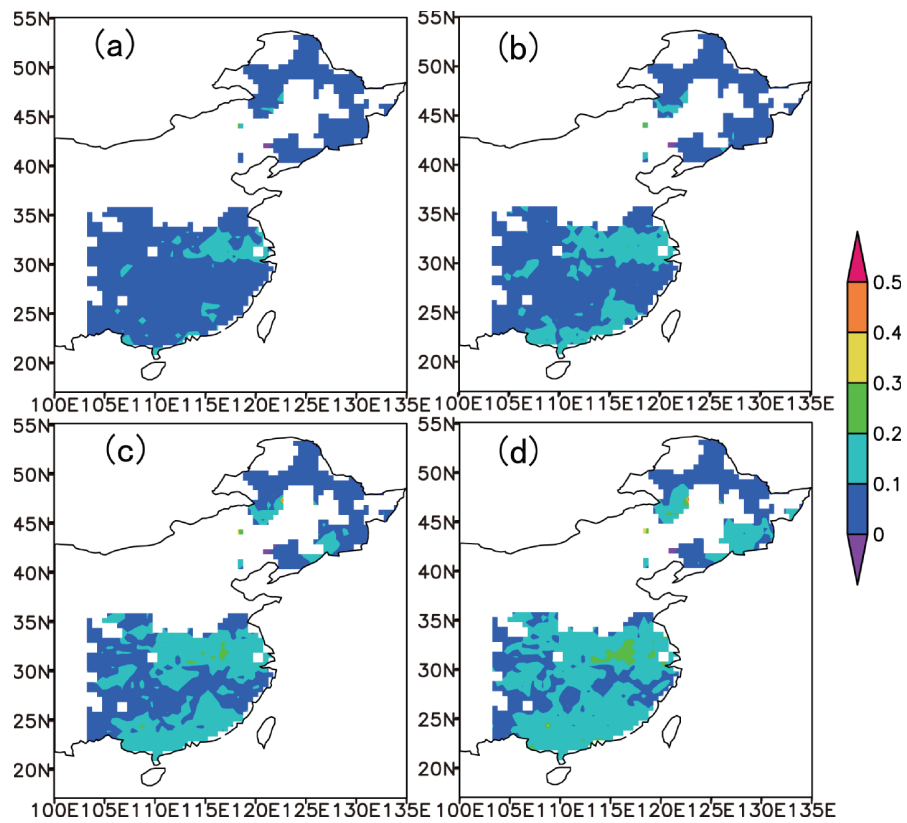


**Fig. 4.** Average relative change in NPP during 1961–1970 (units:  $\text{g C m}^{-2} \text{yr}^{-1}$ ): (a)  $\delta=0.5$ , (b)  $\delta=0.6$ , (c)  $\delta=0.7$ , (d)  $\delta=0.8$ .

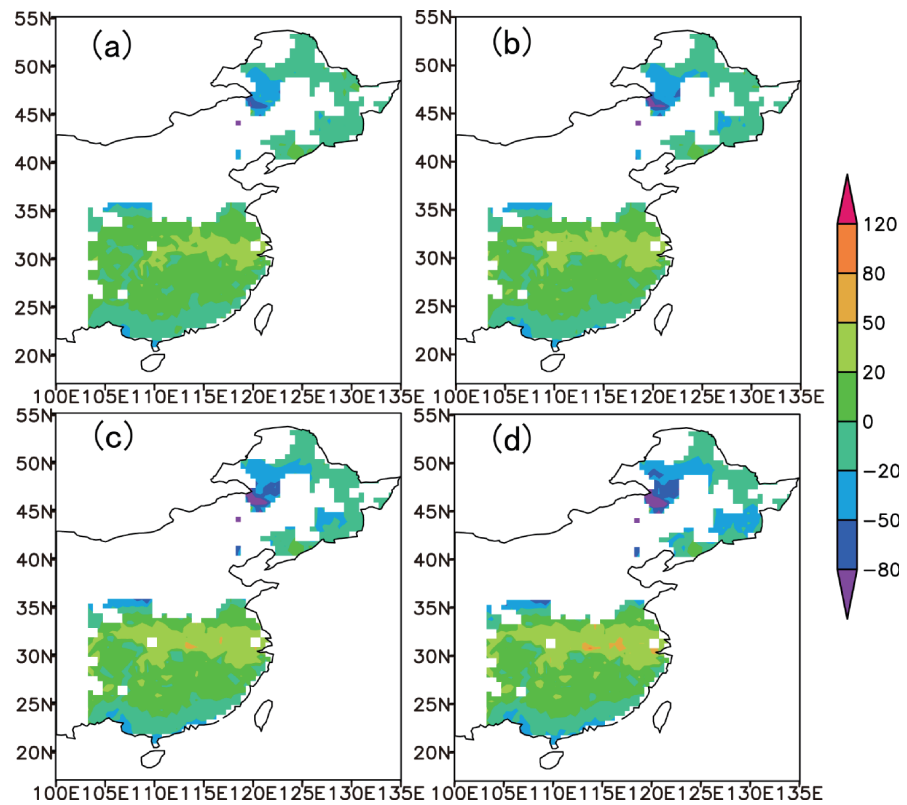


**Fig. 5.** Same as in Fig. 3, but for GPP (units:  $\text{g C m}^{-2} \text{yr}^{-1}$ ).

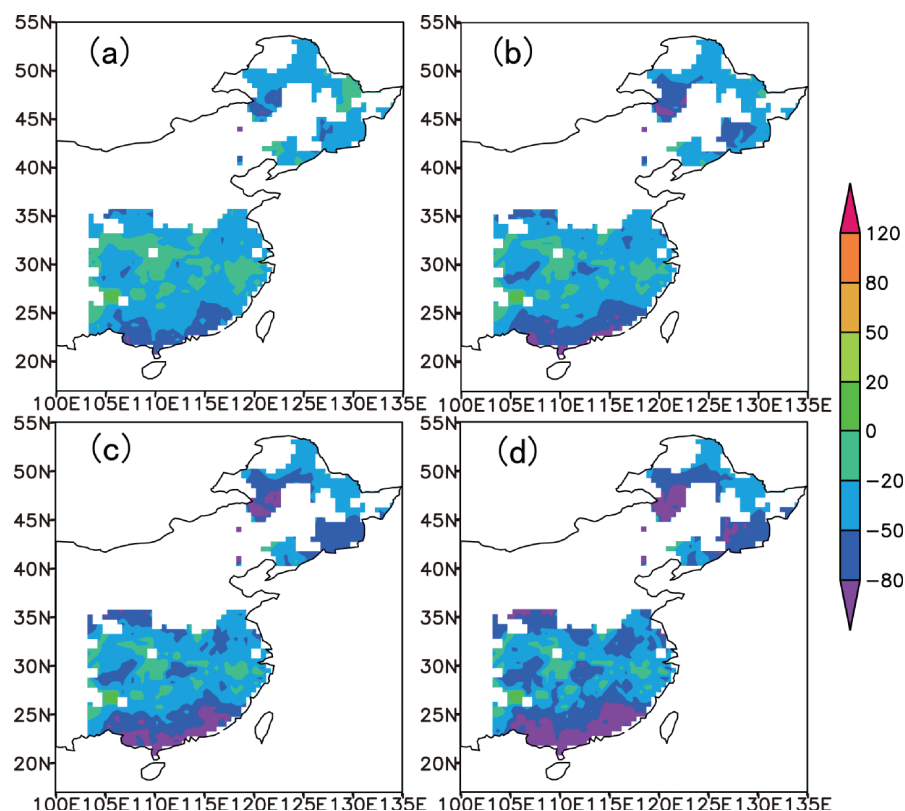


Fig. 6. Same as in Fig. 3, but for Ra (units:  $\text{g C m}^{-2} \text{ yr}^{-1}$ ).

China, where boreal needle-leaved summergreen (BoNS) or boreal broad-leaved summergreen (BoBS) substitutes for BoNE when deforestation occurs. These results show that the plant cover of BoNS or BoBS was larger than that of BoNE when deforestation occurred. Although the plant cover in southern China also underwent changes, plants remain fixed. Within the LPJ model, the interaction between the climate condition and vegetation was not considered. The variations in vegetation amount could not cause the climate change, so the plant scarcely changes.

## 5. Summary

In our study, the different responses of terrestrial ecosystems and carbon cycles to land use in China were investigated under specific conditions by employing the CNOP-I approach within the LPJ model. Our main conclusions are summarized below.

As the extent of deforestation increases, relative change in vegetation amount increases and exhibits nonlinear characteristics. For the same constraint condition parameters, variation in plant amount among the TeBE, the TeBS and the BoNE differed, with a greater variation in northern China than in southern

China. Through an analysis of climate conditions, we demonstrate the cause of variation in the plant amount due to deforestation. Within a certain extent of land use, NPP increased for the whole region. The reasons for the increase were different for the three PFTs. Both GPP and Ra were reduced for TeBE and BoNE, but NPP was augmented because the decrease in GPP was less than that of Ra. However, in the case of TeBS, NPP was augmented because GPP increased and Ra decreased. Furthermore, the PFT basically remains changeless on the whole region due to the small amount of loss in leaf carbon mass. The deforestation of the plant trees is important mode of the land use. When deforestation occurs, plants have the ability to regrow with proper precipitation and the temperature. The regrowth ability for different trees varies. For example, in the southern China, adequate precipitation and sunlight facilitate the robust regrowth of trees. However, in northern China, the temperature is low, regrowth is weaker than in the southern China. The CNOP approach could post the difference in the different trees.

Data have been available on land use and land use changes; however, we did not employ them in our research. Instead, we have produced experimental re-



sults by employing a nonlinear optimization method from the perspective of the initial perturbation to reveal the maximum variations in the vegetation amount related to a certain extent of land use. We chose the study period 1961–1970 to investigate the variation in terrestrial ecosystem due to land use because human activities intensified during this time and the climate data are credible for this period. Our study did not consider variation in the response of terrestrial ecosystems to land use. In northern China, the climate condition abruptly changes in the late 1970s. The impact of human activities on the terrestrial ecosystem during the last 1970s, 1980s, and 1990s is worthy of discussion. The variations in net ecosystem production (NEP) and/or soil carbon also fail to discuss due to land use, especially for carbon source and sink. These variations will be discussed in a future analysis.

**Acknowledgements.** Funding was provided from the State Key Development Program for Basic Research (Grant No. 2012CB955202), National Natural Science Foundation of China (Grant Nos. 40905050 and 40830955) and the KZCX3-SW-230 of the Chinese Academy of Sciences (CAS).

## REFERENCES

- Beer, C., W. Lucht, D. Gerten, K. Thonicke, and C. Schmullius, 2007: Effects of soil freezing and thawing on vegetation carbon density in Siberia: A modeling analysis with the Lund-Potsdam-Jena Dynamic Global Vegetation Model (LPJ-DGVM). *Global Biogeochemical Cycles*, **21**, GB1012, doi: 10.1029/2006GB002760.
- Bernoux, M., M. C. S. Carvalho, B. Volkoff, and C. C. Cerri, 2001: CO<sub>2</sub> emission from mineral soils following land-cover change in Brazil. *Global Change Biology*, **7**, 779–787.
- Betts, A. K., and J. H. Ball, 1997: Albedo over the boreal forest. *J. Geophys. Res.*, **102**, 28901–28909, doi: 10.1029/96JD03876.
- Birgin, E. G., J. M. Martinez, and M. Raydan, 2000: Nonmonotone spectral projected gradient methods for convex sets. *SIAM Journal on Optimization*, **10**, 1196–1211.
- Bonan, G., S. Levis, S. Sitch, M. Vertenstein, and K. Oleson, 2003: A dynamic global vegetation model for use with climate models: Concepts and description of simulated vegetation dynamics. *Global Change Biology*, **9**, 1543–1566.
- Brovkin, V., S. Sitch, von W. Bloh, M. Claussen, E. Bauer, and W. Cramer, 2004: Role of land cover changes for atmospheric CO<sub>2</sub> increase and climate change during the last 150 years. *Global Change Biology*, **10**, 1253–1266, doi: 10.1111/j.1365-2486.2004.00812.x.
- Claussen, M., V. Brovkin, and A. Ganopolski, 2001: Biogeophysical versus biogeochemical feedbacks of large-scale land cover change. *Geophys. Res. Lett.*, **28**, 1011–1014, doi: 10.1029/2000GL012471.
- Conant, R. T., and K. Paustian, 2002: Potential soil carbon sequestration in overgrazed grassland ecosystems. *Global Biogeochemical Cycles*, **16**, 1143, doi: 10.1029/2001GB001661.
- Conant, R. T., K. Paustian, and E. T. Elliott, 2001: Grassland management and conversion into grassland: Effects on soil carbon. *Ecological Applications*, **11**, 343–355.
- Cramer, W., and Coauthors, 2001: Global responses of terrestrial ecosystem structure and function to CO<sub>2</sub> and climate change: Results from six dynamic global vegetation models. *Global Change Biology*, **7**, 357–373.
- Dan, L., J. Ji, and Y. He, 2007: Use of ISLSCP II data to intercompare and validate the terrestrial net primary production in a land surface model coupled to a general circulation model. *J. Geophys. Res.*, **112**, D02S90, doi: 10.1029/2006JD007721.
- DeFries, R. S., C. B. Field, I. Fung, G. J. Collatz, and L. Bounoua, 1999: Combining satellite data and biogeochemical models to estimate global effects of human-induced land cover change on carbon emissions and primary productivity. *Global Biogeochemical Cycles*, **13**, 803–815, doi: 10.1029/1999GB900037.
- Fang, J. Y., A. P. Chen, C. H. Peng, S. Q. Zhao, and L. J. Ci, 2001: Changes in forest biomass carbon storage in China between 1949 and 1998. *Science*, **292**, 2320–2322.
- Foley, J. A., and Coauthors, 2005: Global Consequences of Land Use. *Science*, **309**, 570–574.
- Gao, Q., X. B. Li, and X. S. Yang, 2003: Responses of vegetation and primary production in north-south transect of eastern China to global change under land use constraint. *Acta Botanica Sinica*, **45**, 1274–1284.
- Ge, Q. S., J. H. Dai, F. N. He, Y. Pan, and M. M. Wang, 2008: Land use changes and their relations with carbon cycles over the past 300 a in China. *Science in China (D)*, **51**, 871–884.
- Global Carbon Project, 2003: Science framework and implementation. Earth System Science Partnership (IGBP, IHDP, WCRP, DIVERSITAS) Report No. 1, Global Carbon Project Report No. 1, Canberra, 69pp.
- Global Land Project, 2005: Science plan and implementation strategy. IGBP Report No. 53/IHDP Report No. 19, IGBP Secretariat, Stockholm, 64pp.
- Houghton, R. A., 1995: Land-use change and the carbon cycle. *Global Change Biology*, **1**, 275–287.
- Houghton, R. A., and J. L. Hackler, 2003: Sources and sinks of carbon from land-use change in China. *Global Biogeochemical Cycles*, **17**, 1034, doi: 10.1029/2002GB001970.
- Jiang, Z. N., and M. Mu, 2009: A comparisons study of the methods of conditional nonlinear optimal perturbations and singular vectors in ensemble prediction. *Adv. Atmos. Sci.*, **26**, 465–470, doi: 10.1007/s00376-

- 009-0465-6.
- Jung, M., and Coauthors, 2007: Uncertainties of modeling gross primary productivity over Europe: A systematic study on the effects of using different drivers and terrestrial biosphere models. *Global Biogeochemical Cycles*, **21**, GB4021, doi: 10.1029/2006GB002915.
- Kicklighter, D. W., and Coauthor, 1999: A first-order analysis of the potential role of CO<sub>2</sub> fertilization to affect the global carbon budget: A comparison of four terrestrial biosphere models. *Tellus B*, **51**, 343–366.
- Lambin, E. F., and H. J. Geist, Eds., 2006: *Land-Use and Land-Cover Change*. Vol. 18, *Local Processes and Global Impacts*, Global Change—The IGBP Series, Springer-Verlag, Berlin, 222pp.
- Mitchell, T. D., and P. D. Jones, 2005: An improved method of constructing a database of monthly climate observations and associated high-resolution grids. *International Journal of Climatology*, **25**, 693–712.
- Mu, M., and B. Wang, 2007: Nonlinear instability and sensitivity of a theoretical grassland ecosystem to finite-amplitude perturbations. *Nonlinear Processes in Geophysics*, **14**, 409–423.
- Mu, M., and Z. N. Jiang, 2008: A new approach to the generation of initial perturbations for ensemble prediction: Conditional nonlinear optimal perturbation. *Chinese Science Bulletin*, **53**, 2062–2068.
- Mu, M., W. S. Duan, and B. Wang, 2003: Conditional nonlinear optimal perturbation and its applications. *Nonlinear Processes in Geophysics*, **10**, 493–501.
- Mu, M., L. Sun, and H. A. Dijkstra, 2004: The sensitivity and stability of the ocean's thermohaline circulation to finite amplitude perturbations. *J. Phys. Oceanogr.*, **34**, 2305–2315.
- Mu, M., F. Zhou, and H. Wang, 2009: A method for identifying the sensitive areas in targeted observations for tropical cyclone prediction: Conditional nonlinear optimal perturbation. *Mon. Wea. Rev.*, **137**, 1623–1639.
- Mu, M., W. S. Duan, Q. Wang, and R. Zhang, 2010: An extension of conditional nonlinear optimal perturbation approach and its applications. *Nonlinear Processes in Geophysics*, **17**, 211–220, doi: 10.5194/npg-17-211-2010.
- Ni, J., and X. S. Zhang, 2000: Climate variability, ecological gradient and the Northeast China Transect (NSTEC). *Journal of Arid Environments*, **46**, 313–325.
- Petit, C. C., and E. F. Lambin, 2002: Long-term land-cover changes in the Belgian Ardennes (1775–1929): Model-based reconstruction vs. historical maps. *Global Change Biology*, **8**, 616–630.
- Piao, S., J. Fang, L. Zhou, K. Tan, and S. Tao, 2007: Changes in biomass carbon stocks in China's grasslands between 1982 and 1999. *Global Biogeochemical Cycles*, **21**, GB2002, doi: 10.1029/2005GB002634.
- Prentice, I. C., W. Cramer, S. P. Harrison, R. Leemans, R. A. Monserud, and A. M. Solomon, 1992: A global biome model based on plant physiology and dominance, soil properties and climate. *Journal of Biogeography*, **19**, 117–134.
- Quaife, T., S. Quegan, M. Disney, P. Lewis, M. Lomas, and F. I. Woodward, 2008: Impact of land cover uncertainties on estimates of biospheric carbon fluxes. *Global Biogeochemical Cycles*, **22**, GB4016, doi: 10.1029/2007GB003097.
- Sitch, S., and Coauthor, 2003: Evaluation of ecosystem dynamics, plant geography and terrestrial carbon cycling in the LPJ dynamic global vegetation model. *Global Change Biology*, **9**, 161–185.
- Sitch, S., V. Brovkin, W. von Bloh, D. van Vuuren, B. Eickhout, and A. Ganopolski, 2005: Impacts of future land cover changes on atmospheric CO<sub>2</sub> and climate. *Global Biogeochemical Cycles*, **19**, GB2013, doi: 10.1029/2004GB002311.
- Solomon, D., and Coauthor, 2007: Long-term impacts of anthropogenic perturbations on the dynamics and speciation of organic carbon in tropical forest and subtropical grassland ecosystems. *Global Change Biology*, **13**, 511–530.
- Sun, G. D., and M. Mu, 2009: Nonlinear feature of the abrupt transitions between multiple equilibria states of an ecosystem model. *Adv. Atmos. Sci.*, **26**, 293–304, doi: 10.1007/s00376-009-0293-8.
- Vitousek, P. M., H. A. Mooney, J. Lubchenco, and J. M. Melillo, 1997: Human domination of earth's ecosystems. *Science*, **277**, 494–499.
- Wen, X. Y., S. W. Wang, J. H. Zhu, and D. Viner, 2006: An overview of China climate change over the 20th century using UK UEA/CRU high resolution grid data. *Chinese J. Atmos. Sci.*, **30**, 894–904. (in Chinese)
- Wu, H. B., Z. T. Guo, and C. H. Peng, 2003: Land use induced changes of organic carbon storage in soils of China. *Global Change Biology*, **9**, 305–315.
- Zobler, L., 1986: A world soil file for global climate modelling. NASA Technical Memorandum, 87802, 32pp.